An Effective Medical Image Classification: Transfer Learning Enhanced by Auto Encoder and Classified with SVM

Omer Sevinc[1], Mehrube Mehrubeoglu[2], Mehmet Serdar Guzel[3*], Iman Askerzade[3]

[1] Computer Programming, Ondokuz Mayis University, Vezirkopru 55900, Samsun, Turkey
[2] Texas A&M University-CC, 6300 Ocean Dr., Corpus Christi 78412, TX, USA
[3] Dept. of Computer Engineering, Ankara University, Golbasi 06830, Ankara, Turkey

Corresponding Author Email: mguzel@ankara.edu.tr

ABSTRACT

The count of white blood cells is vital for disease diagnosis, which is exploited to identify many diseases like infections and leukemia. COVID-19 is another critical disease which should be detected and cured immediately. These diseases are better diagnosed using radiological and microscopic imaging. A clinical experience is required by a physician, to identify and classify the Chest X-rays or the microscopic blood cell images. In this study a novel approach is proposed for classifying medical images by using transfer learning method which is ResNet-50 where features are reduced with Auto Encoder (AE) and classified with a Support Vector Machine (SVM) instead of softmax classifier which is tested with different optimizers. The proposed method is compared with VGG-16 and ResNet-50, Inception-V3 which use softmax classifiers. Experimental results indicated that the proposed method possess 97.3% and 99% accuracy on WBC and COVID-19 datasets respectively which are higher than compared methods for each dataset.

1. INTRODUCTION

White blood cells called leukocytes play a critical role to identify many health problems like leukemia, AIDS and cancer [1]. The count of the white blood cells in the bloodstream gives some hints on a person's immune system together with the possible health threats [2]. White blood cells (WBC) are divided into subtypes as lymphocytes, monocytes, eosinophils, and neutrophils [3, 4]. The latest COVID-19 virus has been very contagious, spreading so fast all around the world, and affecting the daily lives of the majority of people. The preliminary identification of COVID-19 is paramount for health specialists to end slow the epidemic curve [5]. The known diagnostic tests need hardware and equipment, and mostly have relatively lower sensitivity. Chest X-ray images were used for identifying COVID-19 successfully [6]. In this study, the dataset collection of chest X-ray images were used to automatically detect the COVID-19 disease fast and accurately [7].

The study presented in this paper compares the best transfer learning models proposed over continuing years for medical image classification. The proposed model provides a novel approach to the WBC and Chest X-ray classification problems to count the subtypes of blood cells and identify the patients as normal or with COVID-19.

Three architectures, namely, visual geometry group (VGG16) [8], ResNet-50 [9], and Inception-V3 were implemented for feature extraction to classify cells from WBC and chest X-rays in the study.

The proposed model has been enhanced by handling the features from transfer learning which were then reduced by auto encoder, tested with Adam, RmsProp, and Adadelta optimizers, and finally classified with SVM classifier. The results show prominent accuracy results of about 99% for COVID-19 and 97.3% for WBC classification, respectively. These results demonstrate that the proposed model has better accuracy than the other compared models. The rest of this paper includes related work (Section 2), methods (Section 3), experiments and results (Section 4), conclusions (Section 5), and References, respectively.

2. RELATED WORKS

Pre-trained CNN model ResNet [10] has been so effective and efficient that it has proved to be one of the featured models in competitions. The acquired parts of the images through layers by the deep CNN models are effectively learned and inferences made fully from the details [11]. Thus, the model can accurately classify the images [12] being studied. Incremental layer numbers in the model improves the capability of representing features of image in theory; therefore, it can be concluded that more layers could potentially result in improved network architectures that can work successfully.

Other studies have been compared with the proposed model which use the similar benchmark datasets [13]. Compared models use the white blood cell data set and chest X-rays on Kaggle with hybrid CNN and RNN models for classifying blood cells and X-rays [14].

Additionally, pre-trained CNN architectures were trained on medical images through transfer learning. To classify MRI and PET, the proposed model succeeded an accuracy rate over 90%. Liang et al. used the divNet architecture in their proposed method [15]. Another classification made based on an ordinary machine learning algorithm involved identifying

from features weather a patient had Alzheimer's disease or not. SqueezeNet proposed that it could be considered a light CNN model for COVID-19 classification from CT images with about 88% accuracy in classification success [16]. Custom CNN models are run on medical images and about 94% accuracy results have been reported [17]. A CNN-LSTM model was used to classify COVID-19 with a 98% accuracy. The method uses the extracted features from CNN to diagnose COVID-19 with LSTM to increase the classification success rate [18]. In another study for nodule detection in lung CT images, CNN models were designed for nodule detection and about 97% accuracy was achieved [19]. Finally, Hamidian et al. uses CNN-AE for COVID-19 diagnosis and reported 96.05% accuracy [20]. The proposed model here combines auto encoder and SVM classifier on ResNet-50 and evaluates the optimizers to provide higher accuracy results on both WBC and chest X ray images.

3. METHODS

3.1 Transfer learning

Inadequate image datasets can exploit the advantage of transfer learning where learned parameters handled from the pre-trained CNN models. The pre-trained models are set and started with ImageNet weights and trained with the dataset for white blood cells and COVID-19 X-rays and the classification results were handled respectively. The datasets are publicly open on Kaggle which are commonly used. A pretrained model has the advantage of allowing you to use weights that are already calibrated to make predictions.

For achieving the goal, on the pre-trained model the convolutional layers are frozen, where the fully connected (FC) layers are trained all over on the clinical dataset. The dataset for WBC and Chest X-Ray for COVID-19 are labeled dataset where 80% of each dataset are used to train over FC layers as supervised models. The pretrained model has the advantage of using weights that are already calibrated to make classifications. After freezing the layers and make some of them trainable the rest of the layers trained with the datasets.

The logic beyond the transfer learning is that even if clinical datasets differentiate from non-clinic datasets, the lower features are common for most of the images [21]; therefore, conveyed parameters can serve as a representative set of features that decrease the requirement for a huge dataset as well as the training duration and memory cost [22].

3.2 VGG, ResNet, inception

The Visual Geometry Group established VGG-16 in ILSVRC2014 which were then one of two prospering models on ImageNet [23]. The improvements came into play by changing large kernel-sized filters of AlexNet with many small sized kernel filters which resulted in convolution layers of 16 and 13 for VGG-16 and VGG-13 respectively. One of the problems with increased layers in CNN models can involve vanishing gradients and overfitting issues. The approach of residual learning allowed the ResNet model to create a solution for this issue. Apart from other prior CNN models, residuals are learnt from input for each convolution layer by ResNet instead of features. This is achieved by using a theme called identity shortcut connections [24]. Different ResNet models use a varied amount of layers, like ResNet-50, ResNet-

34. The Inception-V1 model attempted to enhance the efficiency of VGGNet by reducing the memory utilization and execution time without reducing accuracy [25]. This is achieved by eliminating the repeating or zero activation functions of VGGNet. Thus, GoogLeNet came with a new module addition named as Inception that steps up sparse connections between the activation functions. Architecture was tuned after Inception-V1 in three sub versions in the following years. Batch normalization was exploited with Inception-V2 for training [26]. The factorization method was introduced with Inception-V3 to enhance the computational complexity [27].

3.3 Auto encoder

AE is an unsupervised model. It compresses the data into lower dimensions to encode and decodes to reconstruct the original data. The compressed representation of the input is held in the bottleneck layer. So, the amount of output units has to be equal to the amount of inputs while the input data is reconstructed [28]. In general AE is made up of an encoder and a decoder. The encoder compresses by lowering the dimension of input into the bottleneck layer, and the decoder reconstructs original input from compressed data [29, 30].

3.4 SVM

Linearly separable and linearly inseparable problems can be solved with SVM depending on the type of the kernel used. 'Linear', 'Polynomial', 'rbf' kernels can be selected according to the problem and the task to be performed. The role of the SVM is to assist with the selection of optimal decision boundaries or hyperplanes [31] to solve numerous tasks as a classifier. Vapnik constructed a linear classifier for the original maximum margin hyperplane algorithm. However, an approach to create nonlinear classifiers by implementing the kernel trick was suggested by him and his friends [32] to handle maximum margin hyperplanes [33]. The SVM formula to specify hyperplanes for nonlinear classification can be seen in Eq. (1). One of the important parts in SVM is to use regularization and hinge loss which is implemented with Eq. (2) and Eq. (3) [34].

$$\lambda \|w\|^2 + \left[\frac{1}{n} \sum_{i=1}^{n} \max(0, 1 - y_i \, (w^T \, x_i - b)) \right] \qquad (1)$$

$$\hat{f} = \arg_{f \epsilon \mathcal{H}}^{min} \, \hat{\in} \, (f) + \mathcal{R}(f) \qquad (2)$$

$$\left[\frac{1}{n} \sum_{i=1}^{n} \max(0, 1 - y_i \, (w^T \, x - b)) \right] + \lambda \|w\|^2 \qquad (3)$$

3.5 Proposed model

In the proposed model, one of the most prominent pre-trained transfer learning methods Resnet50 used for testing and training the clinical images to classify correctly. But the enhanced points are the dropouts used effectively to implement auto encoders to reduce the features. Reducing the features increases learning rate but decreases overfitting. The optimizers are given into an array to test separately to evaluate accuracy performance for the classification. The Adam, which

is the best optimizer for image classification on deep CNN architectures compared with Rmsprop and Adadelta optimizers. At the FC layer (Fully connected) features were retrieved from Fc1000 layer, which is the layer before the Softmax layer of Resnet50 models. In the model it was chosen to freeze some layers which doesn't change weights but provides time saving and computational cost, and trainable layers were added. Then, the pretrained model connected to the trainable layers of our model. It is done by using a flatten layer to connect the dimensions of the previous layers with the trainable layers. Autoencoder had the role of feature reduction which provides a smaller feature subset from the entire feature sets. Auto encoder is implemented by adding dense layers before FC layer to encode and bring the features to the bottleneck to reduce the size of them. In the model implementation it was made by adding Dense layers as to reduce the number of features.

The classification amounts were written for the feature vector of dimension (12,512 x 1000) was obtained for WBC and (1700 x 1000) for Chest X Ray respectively. The model ran separately for each dataset that connected to FC layer which represented as 1000 features. For the classification of WBC the categorical classification is used to result with 4 different type of class, and binary classification is used to classify COVID-19 dataset into positive or negative. The model ran on WBC and COVID-19 X-ray datasets separately so first model is trained to deal with WBC and outputs are handled then same steps implemented for X-ray dataset and the model trained for handling different features. At classification stage with Softmax classifier, the images are classified. After running the prominent pre-trained models on medical images, the accuracy results are compared. When the SVM was attached to the FC layer had better classification accuracy over softmax classifier and it was claimed that the SVM-based models can lower classification error than the Softmax-based models [35]. After running the prominent pre-trained models on medical images, the accuracy results are compared. The results showed over 93% accuracy. However, it is obviously seen that if the pre-trained models are fine-tuned with feature reductions, switched with different optimizers, and tested with different classifiers, accuracy results can be improved. So, the enhanced structure was introduced to the proposed model which gave better accuracy results. After handling the feature sets, they were sent to the SVM classifier instead of Softmax to get improved classification with higher accuracy results. The proposed model diagram, the ResNet-50-AE-SVM can be seen on Figure 1.
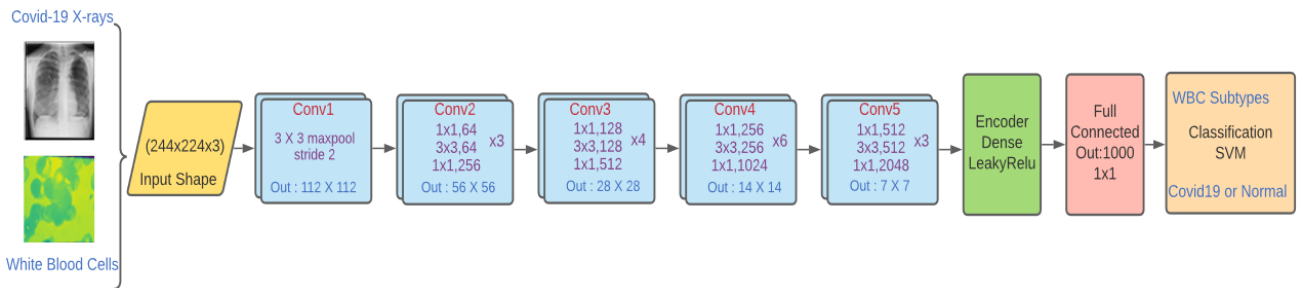

Figure 1. The proposed model resnet50+AE+SVM

3.6 Dataset

In this study WBC dataset [36] and chest X-rays [37] are used on publicly available websites. WBC data set includes 12.500 images that contains about 3000 images for each of eosinophils, lymphocytes, monocytes, and neutrophils. Chest X-rays dataset has 1700 images consists of 350 COVID-19 positive and 1350 normal images. WBC and COVID-19 images were classified into 4 classes (12500, 4) and 2 classes (1700,2). For training %80, and for the test and validation %20 of each dataset were used. The images are preprocessed with Keras, they were resized and turned shapes of the images into (224, 224, 3). Then the images were converted into to np array (1, 224, 224, 3) and normalized.

Sample of COVID -19 chest X ray images can be seen on the Figure 2. The WBC blood subtypes can be seen on Figure 3 as below.
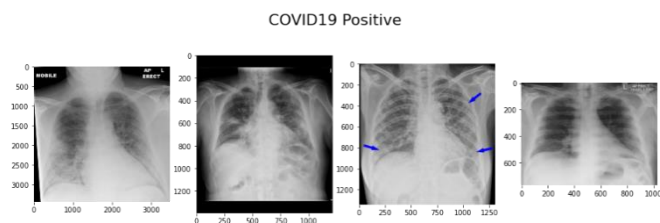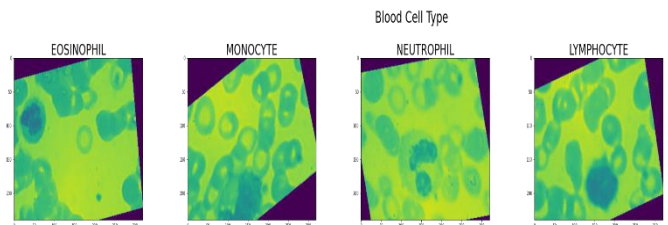

Figure 3. The blood cell types

4. EXPERIMENTS AND RESULTS

The proposed ResNet-50-AE-SVM model was run on a computer with i7 processor, 32 GB RAM, and through Kaggle cloud servers. The SVM classifier was tested using the rbf kernel. Other transfer learning models which are VGG-16, ResNet-50 and Inception-V3 were used for the comparison of the experimental results and accuracies. In the proposed framework, ResNet was used for feature extraction. The top layers of the model were disabled and modified with custom dense layers to train the sample images. Features were reduced with AE which were applied through and after the dense layers to select the most relevant features and reduce overfitting. The optimizers Adam, Rmsprop and Adadelta were added in an array into the model to test each separately. Relu is used for the activation function which gives best results. The loss

Figure 2. COVID-19 sample X-ray positive results

function for WBC and COVID-19 classifications are used as categorical and binary cross entropy, respectively. However, to implement SVM on Resnet50 hinge loss function and l2 regularization are used.

By using regularizers and loss functions the SVM classifier was implemented at the fully connected stage of the model to get better classification accuracy results.

Other transfer learning models were also used on the sample data set for comparison. The top layers were disabled from the VGG-16, ResNet-50 and Inception-V3, and instead, custom layers were added at the top of the model to train the sample dataset. The images were classified with the Softmax classifier at the end. As shown in Table 1, the highest performance was shown by the introduced ResNet-50-AE-SVM model with an accuracy rate of 97.3% for WBC and 99% for chest X-rays in COVID-19 classification. Execution time and accuracy rates of proposed model and other transfer learning models are given in the Table 1, too. The accuracy and loss values during the epoch is shown in Figure 4 and Figure 5 for WBC and COVID-19 classification, respectively. Figure 6 shows the confusion matrix values for the WBC and the COVID-19 classification from left to right. Table 2 represents the accuracy with different optimizers on the proposed ResNet-50-AE-SVM model. It can be understood from the figure and tables the proposed model has an accuracy rate of 97.3% on WBC and 99.0% on chest X-rays which are better than state-of-the-art transfer learning models. The proposed model had an optimum execution time with the highest classification accuracies. It is obvious that the ResNet-50, VGG-16 and Inception-V3 models also performed well with accuracy over 93%, although not as highly as the proposed ResNet-50-AE-SVM model. The accuracy, f1-score, precision and recall values of the proposed model can be seen in Table 2 and Table 3.
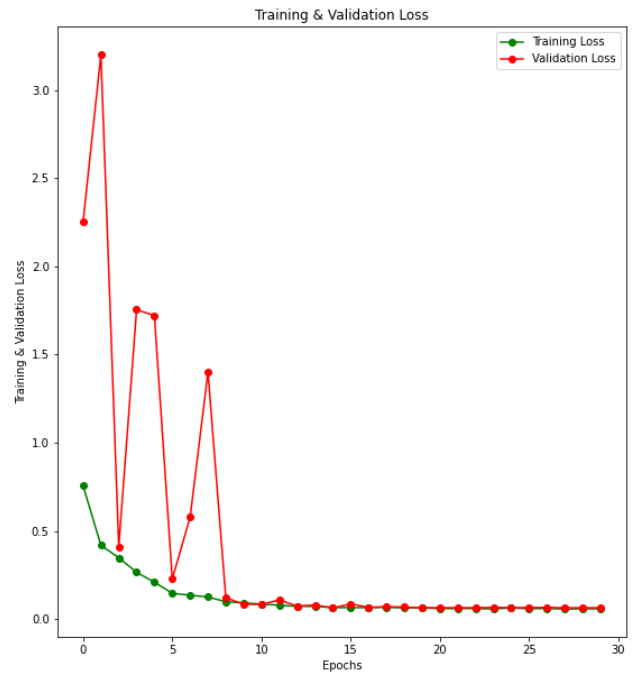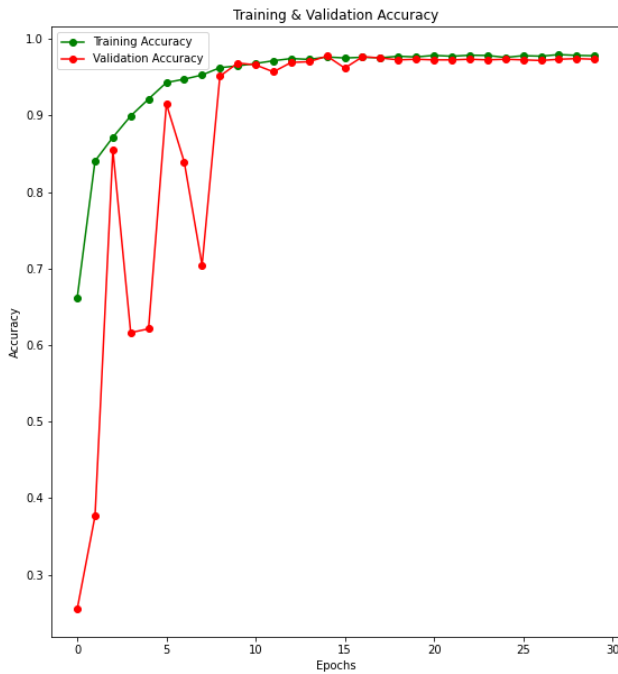

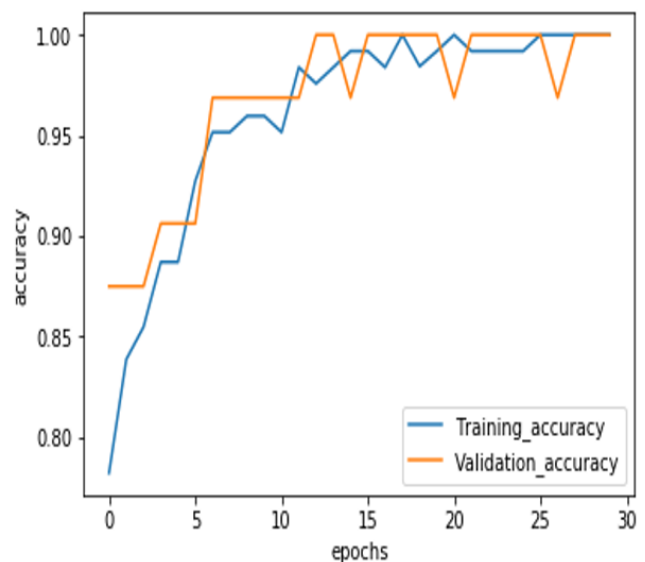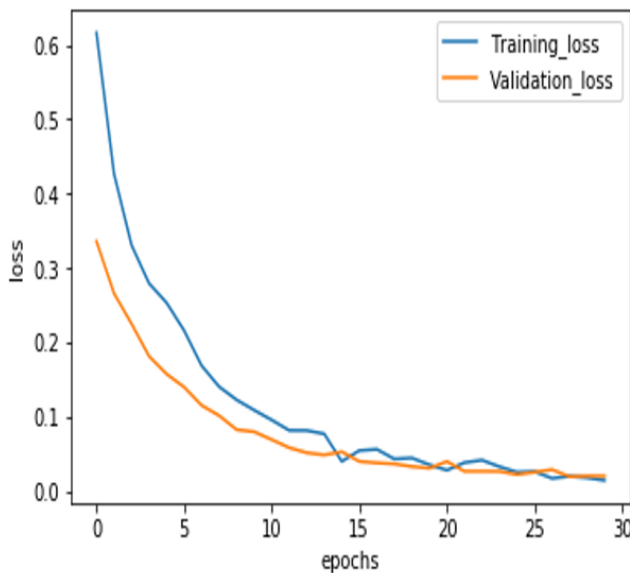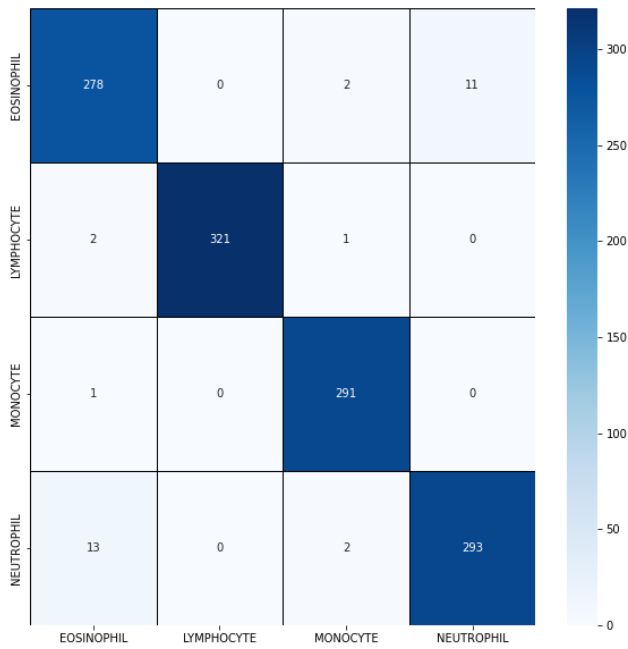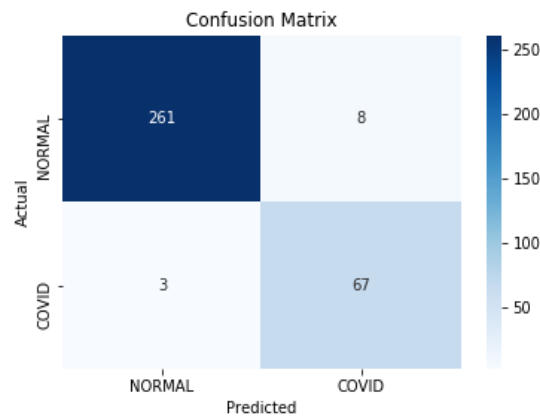**Figure 4.** WBC loss and accuracy for training and the validation results

Figure 5. COVID-19 loss and accuracy for training and the validation results

| (a) WBC confusion matrix | (b) COVID-19 confusion matrix |

Figure 6. Proposed method confusion matrix for WBC (a) and COVID-19 (b)

Table 1. Comparison of the accuracy results for proposed and other methods

Dataset	Method	Average execution time (s)	Test accuracy (%)
WBC	VGG16	3090.53	%93.4
COVID-19 X rays	VGG16	1720.10	%95.1
WBC	Resnet50	1210.90	%94.2
COVID-19 X rays	Resnet50	1121.25	%96.2
WBC	Inception-V3	2090	%93.2
COVID-19 X rays	Inception-V3	1688	%94.7
WBC	Resnet50+AE+SVM (Proposed)	1250.32	**%97.2**
COVID-19 X rays	Resnet50+AE+SVM (Proposed)	1123.45	**%99**

Table 2. f1-score and other metrics for each subtypes of WBC

WBC	Precision	Recall	f1 Score	Support
Eosinophil	0.95	0.95	0.96	310
Lymphocyte	0.98	1.00	0.99	320
Monocyte	1.00	0.98	0,98	327
Neutrophil	0.95	0.94	0.96	295
accuracy value			0.97	1252
weighted average	0.98	0.97	0.97	1252

Table 3. f1-score and other metrics for COVID-19

COVID-19	Precision	Recall	f1 Score	Support
normal	0.99	0.98	0.99	269
positive	0.98	0.96	0.97	70
accuracy value			0,99	339
weighted average	0.98	0.98	0.98	339

5. CONCLUSIONS

The proposed model, which is the ResNet-50-AE-SVM with Adam optimizer based on convolutional neural networks, feature extraction and reduction to improve classification accuracy where it has a considerable execution time. In transfer learning models CNN architectures are very deep which contain convolutional and dense blocks to get detailed features from the images for better detection and classification. However, by enhancing the transfer learning models with feature reductions through and after dense layers, combined with testing with different optimizers and classifiers, increases the learning, and decreases overfitting and classification time. In the proposed models, the Adam, RmsProp and Adadelta optimizer are tested separately. The auto encoders used to reduce features through dense layers. At the last stage, the SVM classifier is implemented which is one of the most effective classifiers for this application. Other transfer learning models which are VGG-16, ResNet-50 and Inception-V3 were run on the same datasets where the default structures were used with Softmax classifiers, but only top layers disabled to modify with custom dense layers and train on the sample datasets. The accuracy results from the models were over 93% which are considerably good, but the proposed method showed even better accuracy results. The proposed novel approach is based on AE, different optimizers and SVM, can train on extracted features and carry out accurate and fast classification of medical images of WBC and chest X-rays. The proposed method demonstrates the most efficient performance with an accuracy rate of 97.3% on classification of WBC subtypes and 99% on Chest X-rays for COVID-19 detection. that the proposed work represents a fast and efficient method for medical image classification. For further studies the CNN model can be replaced with RNN and the medical reports on disease analysis can be evaluated for the text classification of the disease. Some of the hyperparameters can be fine-tuned with optimization algorithms.

Hyperparameters can be fine-tuned with optimization algorithms.

REFERENCES

[1] Joshi, M.D., Karode, A.H., Suralkar, S.R. (2013). White blood cells segmentation and classification to detect acute Leukemia. International Journal of Emerging Trends & Technology in Computer Science (IJETTCS), 2(3): 147-151.

[2] Zhao, J., Zhang, M., Zhou, Z., Chu, J., Cao, F. (2017). Automatic detection and classification of leukocytes using convolutional neural networks. Medical & Biological Engineering & Computing, 55(8): 1287-1301. https://doi.org/10.1007/s11517-016-1590-x

[3] Dean, L. (2005). Blood Groups and Red Cell Antigens. Chapter 1. Bethesda, MD.

[4] Briggs, C. (2009). Quality counts: new parameters in blood cell counting. International Journal of Laboratory Hematology, 31(3): 277-297. https://doi.org/10.1111/j.1751-553X.2009.01160.x

[5] Velavan, T.P., Meyer, C.G. (2020). The COVID-19 epidemic. Tropical Medicine & International Health, 25(3): 278. https://doi.org/10.1111/tmi.13383

[6] Hall, L.O., Paul, R., Goldgof, D.B., Goldgof, G.M. (2020). Finding COVID-19 from chest x-rays using deep learning on a small dataset. arXiv preprint arXiv:2004.02060

[7] Dai, W.C., Zhang, H. W., Yu, J., Xu, H.J., Chen, H., Luo, S.P., Lin, F. (2020). CT imaging and differential diagnosis of COVID-19. Canadian Association of Radiologists Journal, 71(2): 195-200. https://doi.org/10.1177/0846537120913033

[8] Simonyan, K., Zisserman, A. (2014). Very deep convolutional networks for large-scale image recognition. arXiv preprint arXiv:1409.1556.

[9] He, K., Zhang, X, Ren, S, Sun, J. (2016). Deep residual learning for image recognition. In: Proceedings of the IEEE Conference on Computer Vision and Pattern Recognition, pp. 770-778.

[10] Ioffe, S., Szegedy, C. (2015). Batch normalization: Accelerating deep network training by reducing internal covariate shift. arXiv preprint arXiv:1502.03167.

[11] Iglovikov, V., Mushinskiy, S., Osin, V. (2017). Satellite imagery feature detection using deep convolutional neural network: A kaggle competition. arXiv preprint arXiv:1706.06169

[12] Karim, A.M., Güzel, M.S., Tolun, M.R., Kaya, H., Çelebi, F.V. (2019). A new framework using deep auto-encoder and energy spectral density for medical waveform data classification and processing. Biocybernetics and Biomedical Engineering, 39(1): 148-159. https://doi.org/10.1016/j.bbe.2018.11.004

[13] Habibzadeh, M., Krzyżak, A., Fevens, T. (2013). White blood cell differential counts using convolutional neural networks for low resolution images. In International Conference on Artificial Intelligence and Soft Computing, pp. 263-274. https://doi.org/10.1007/978-3-642-38610-7_25

[14] Macawile, M.J., Quiñones, V.V., Ballado, A., Cruz, J.D., Caya, M.V. (2018). White blood cell classification and counting using convolutional neural network. In 2018 3rd International Conference on Control and Robotics Engineering (ICCRE), pp. 259-263. https://doi.org/10.1109/ICCRE.2018.8376476

[15] Liang, S., Sun, R., Lee, J.D., Srikant, R. (2018). Adding one neuron can eliminate all bad local minima. Advances in Neural Information Processing Systems, 31: 4350-4360.

[16] Khagi, B., Kwon, G.R., Lama, R. (2019). Comparative analysis of Alzheimer's disease classification by CDR level using CNN, feature selection, and machine-learning techniques. International Journal of Imaging Systems and Technology, 29(3): 297-310. https://doi.org/10.1002/ima.22316

[17] Polsinelli, M., Cinque, L., Placidi, G. (2020). A light CNN for detecting COVID-19 from CT scans of the chest. Pattern Recognition Letters, 140: 95-100. https://doi.org/10.1016/j.patrec.2020.10.001

[18] Bar, Y., Diamant, I., Wolf, L., Lieberman, S., Konen, E., Greenspan, H. (2015). Chest pathology detection using deep learning with non-medical training. In 2015 IEEE 12th International Symposium on Biomedical Imaging (ISBI), pp. 294-297. https://doi.org/10.1109/ISBI.2015.7163871

[19] Islam, M.Z., Islam, M.M., Asraf, A. (2020). A combined deep CNN-LSTM network for the detection of novel coronavirus (COVID-19) using X-ray images. Informatics in Medicine Unlocked, 20: 100412. https://doi.org/10.1016/j.imu.2020.100412

[20] Hamidian, S., Sahiner, B., Petrick, N. and Pezeshk, A. (2017). 3D convolutional neural network for automatic detection of lung nodules in chest CT. In Medical Imaging 2017: Computer-Aided Diagnosis, 10134: 1013409. https://doi.org/10.1117/12.2255795

[21] Khozeimeh, F., Sharifrazi, D., Izadi, N.H., Joloudari, J.H., Shoeibi, A., Alizadehsani, R., Islam, S.M.S. (2021). Combining a convolutional neural network with autoencoders to predict the survival chance of COVID-19 patients. Scientific Reports, 11(1): 1-18. https://doi.org/10.1038/s41598-021-93543-8

[22] Sharma, S., Mehra, R. (2020). Conventional machine learning and deep learning approach for multi-classification of breast cancer histopathology images—a comparative insight. Journal of Digital Imaging, 33(3): 632-654. https://doi.org/10.1007/s10278-019-00307-y

[23] Weiss, K., Khoshgoftaar, T. M., Wang, D. (2016). A survey of transfer learning. Journal of Big data, 3(1): 1-40.

[24] Simonyan, K., Zisserman, A. (2014). Very deep convolutional networks for large-scale image recognition. arXiv preprint arXiv:1409.1556.

[25] He, K., Zhang, X., Ren, S., Sun, J. (2016). Deep residual learning for image recognition. In Proceedings of the IEEE Conference on Computer Vision and Pattern Recognition, pp. 770-778.

[26] Rhu, M., Gimelshein, N., Clemons, J., Zulfiqar, A., Keckler, S.W. (2016). vDNN: Virtualized deep neural networks for scalable, memory-efficient neural network design. In 2016 49th Annual IEEE/ACM International Symposium on Microarchitecture (MICRO), pp. 1-13. https://doi.org/10.1109/MICRO.2016.7783721

[27] Alamsyah, D., Fachrurrozi, M. (2019). Faster R-CNN with inception v2 for fingertip detection in homogenous background image. In Journal of Physics: Conference Series, 1196(1): 012017. https://doi.org/10.1109/MICRO.2016.7783721

[28] Liu, C.T., Lin, T.W., Wu, Y.H., Lin, Y.S., Lee, H., Tsao, Y., Chien, S.Y. (2018). Computation-performance optimization of convolutional neural networks with redundant filter removal. IEEE Transactions on Circuits

and Systems I: Regular Papers, 66(5): 1908-1921. https://doi.org/10.1109/TCSI.2018.2885953

[29] Pu, Y., Gan, Z., Henao, R., Yuan, X., Li, C., Stevens, A., Carin, L. (2016). Variational autoencoder for deep learning of images, labels and captions. Advances in Neural Information Processing Systems, 29: 2352-2360.

[30] Gondara, L. (2016). Medical image denoising using convolutional denoising autoencoders. In 2016 IEEE 16th International Conference on Data Mining Workshops (ICDMW), pp. 241-246. https://doi.org/10.1109/ICDMW.2016.0041

[31] Karim, A.M., Güzel, M.S., Tolun, M.R., Kaya, H., Çelebi, F.V. (2018). A new generalized deep learning framework combining sparse autoencoder and Taguchi method for novel data classification and processing. Mathematical Problems in Engineering. https://doi.org/10.1155/2018/3145947

[32] Agarap, A.F. (2017). An architecture combining convolutional neural network (CNN) and support vector machine (SVM) for image classification. arXiv preprint arXiv:1712.03541.

[33] Aizerman, M.A. (1964). Theoretical foundations of the potential function method in pattern recognition learning. Automation and Remote Control, 25: 821-837.

[34] Boser, B.E., Guyon, I.M., Vapnik, V.N. (1992). A training algorithm for optimal margin classifiers. In Proceedings of the Fifth Annual Workshop on Computational Learning Theory, pp. 144-152. https://doi.org/10.1145/130385.130401

[35] Fan, J., Lee, J., Lee, Y. (2021). A transfer learning architecture based on a support vector machine for histopathology image classification. Applied Sciences, 11(14): 6380. https://doi.org/10.3390/app11146380

[36] url: https://www.kaggle.com/paultimothymooney/blood-cells, accessed on 15 October 2021.

[37] url: https://www.kaggle.com/tawsifurrahman/COVID-19-radiography-database, accessed on 17 October 2021.